

# A Chiral Gold Nanocluster Au<sub>20</sub> Protected by Tetradentate Phosphine Ligands\*\*

Xian-Kai Wan, Shang-Fu Yuan, Zhi-Wei Lin, and Quan-Ming Wang\*

Dedicated to Professor Xin-Tao Wu on the occasion of his 75th birthday

**Abstract:** The chirality of a gold nanocluster can be generated from either an intrinsically chiral inorganic core or an achiral inorganic core in a chiral environment. The first structural determination of a gold nanocluster containing an intrinsic chiral inorganic core is reported. The chiral gold nanocluster [Au<sub>20</sub>(PP<sub>3</sub>)<sub>4</sub>]Cl<sub>4</sub> (PP<sub>3</sub> = tris(2-(diphenylphosphino)ethyl)phosphine) has been prepared by the reduction of a gold(I)-tetraphosphine precursor in dichloromethane solution. Single-crystal structural determination reveals that the cluster molecular structure has C<sub>3</sub> symmetry. It consists of a Au<sub>20</sub> core consolidated by four peripheral tetraphosphines. The Au<sub>20</sub> core can be viewed as the combination of an icosahedral Au<sub>13</sub> and a helical Y-shaped Au<sub>7</sub> motif. The identity of this Au<sub>20</sub> cluster is confirmed by ESI-MS. The chelation of multidentate phosphines enhances the stability of this Au<sub>20</sub> cluster.

Ligand-protected gold nanoclusters of atomic precision have attracted increasing attention owing to their potential applications in catalysis, sensing, or in biology.<sup>[1–5]</sup> Some gold nanoclusters can bear intrinsically chiral features. The chirality of a gold nanocluster can be generated from two origins: an intrinsically chiral inorganic core or an achiral inorganic core in a chiral environment.<sup>[6]</sup> The environment can be chiral organic ligands or asymmetric arrangements, such as RS-Au-SR-Au-SR staples. A large number of ligand-protected gold nanoclusters have been prepared, but only a few have been structurally determined.<sup>[7]</sup> Au<sub>38</sub>(SR)<sub>24</sub> is chiral owing to the asymmetric arrangement of staples, although it has a high symmetric gold kernel.<sup>[8]</sup> Au<sub>28</sub>(SR)<sub>20</sub><sup>[9]</sup> and Au<sub>102</sub>(SR)<sub>44</sub><sup>[10]</sup> are also chiral for the same reason. However, Au<sub>25</sub>(SR)<sub>18</sub>, having a structure with a Au<sub>13</sub> core surrounded by RS-Au-SR-Au-SR staples, is not chiral.<sup>[11]</sup> Au<sub>36</sub>(SR)<sub>24</sub> is not chiral either.<sup>[12]</sup> To date, there is no structural evidence showing a ligand-protected gold nanocluster with a chiral inorganic core, although a theoretical study confirmed a bare gold cluster Au<sub>34</sub><sup>−</sup> to be intrinsic chiral.<sup>[13]</sup>

Both phosphines and thiolates have been used in the preparation of ligand-protected gold nanoclusters.<sup>[14]</sup> Phosphine-protected gold nanoclusters have a stability issue, because of the weaker Au–P bond in comparison with gold–thiolate bonding. Our strategy to solve this problem is the use of multidentate phosphines, and the attempt with tetradentate phosphine tris(2-(diphenylphosphino)ethyl)phosphine (PP<sub>3</sub>) led to the isolation of a chiral gold nanocluster [Au<sub>20</sub>(PP<sub>3</sub>)<sub>4</sub>]Cl<sub>4</sub> (**1**) with a chiral 20-gold-atom core. Herein, we present this unprecedented structurally determined Au<sub>20</sub> nanocluster with an intrinsic chiral inorganic core. The C<sub>3</sub> Au<sub>20</sub> core can be viewed as the combination of a centered icosahedral Au<sub>13</sub> and a helical Y-shaped Au<sub>7</sub> motif.

The preparation of **1** started with the reduction of [PP<sub>3</sub>Au<sub>4</sub>Cl<sub>4</sub>] by NaBH<sub>4</sub> in CH<sub>2</sub>Cl<sub>2</sub> solution. Solvents were removed to give a black solid, which was recrystallized in CH<sub>2</sub>Cl<sub>2</sub>/CH<sub>3</sub>OH/pentane to afford black crystals of **1** in a typical yield of about 20 %.

Single-crystal structural analysis<sup>[15]</sup> revealed that **1** comprises a tetracationic cluster [Au<sub>20</sub>(PP<sub>3</sub>)<sub>4</sub>]<sup>4+</sup> and chloride counterions. As shown in Figure 1a, the structure has a Au<sub>20</sub> core wrapped by four PP<sub>3</sub> ligands. It has a C<sub>3</sub> symmetry with a threefold axis passing through atoms P1, Au1 and Au8. Geometrically, the Au<sub>20</sub> core can be described as a centered icosahedron Au<sub>13</sub> combined with a Au<sub>7</sub> motif. The Au<sub>20</sub> core has 16 surface and four interstitial gold atoms. Each surface gold atom is coordinated by a phosphorus donor of PP<sub>3</sub>. The PP<sub>3</sub> ligands are of two types: the one on the top bridges four Au atoms symmetrically; the other three are of the same type, each connects one Au<sub>3</sub> triangle and a neighboring Au atom (Figure 1b).

For clarity, the Au<sub>20</sub> core is illustrated in Figure 1c with Au atoms highlighted in different colors. The Y-shaped Au<sub>7</sub> motif is in green and the Au<sub>13</sub> icosahedron is in orange. A side view of the core is illustrated in Figure 1d to show the asymmetric arrangement of gold atoms. As shown in Figure 1e, the 16 surface gold atoms can be classified into six types (from type A to type E). Accordingly, the <sup>31</sup>P NMR should display six peaks at a ratio of 1:3:3:3:3:3 based on the number of atoms of each type. Experimentally, five peaks at δ = 39.78, 41.32, 48.56, 57.05 and 66.26 ppm in a ratio of 1:3:3:6:3 were observed (Supporting Information, Figure S1). The <sup>31</sup>P NMR data match the expected, because the peak at δ = 57.05 ppm actually contains the contribution from phosphorous donors linked to two types of Au atoms (types D and E) with similar coordination environments. The Au–Au distances are in the range of 2.572(2)–3.216(2) Å, and the 2.572(2) Å bond length is among the shortest ones observed for gold clusters. A very

[\*] X.-K. Wan, S.-F. Yuan, Z.-W. Lin, Prof. Dr. Q.-M. Wang  
State Key Lab of Physical Chemistry of Solid Surfaces  
Department of Chemistry, College of Chemistry and  
Chemical Engineering, Xiamen University  
Xiamen, 361005 (P.R. China)  
E-mail: qmwang@xmu.edu.cn

[\*\*] This work was supported by the Natural Science Foundation of China (21125102) and the 973 program (2014CB845603).

Supporting information for this article is available on the WWW under <http://dx.doi.org/10.1002/ange.201308599>.

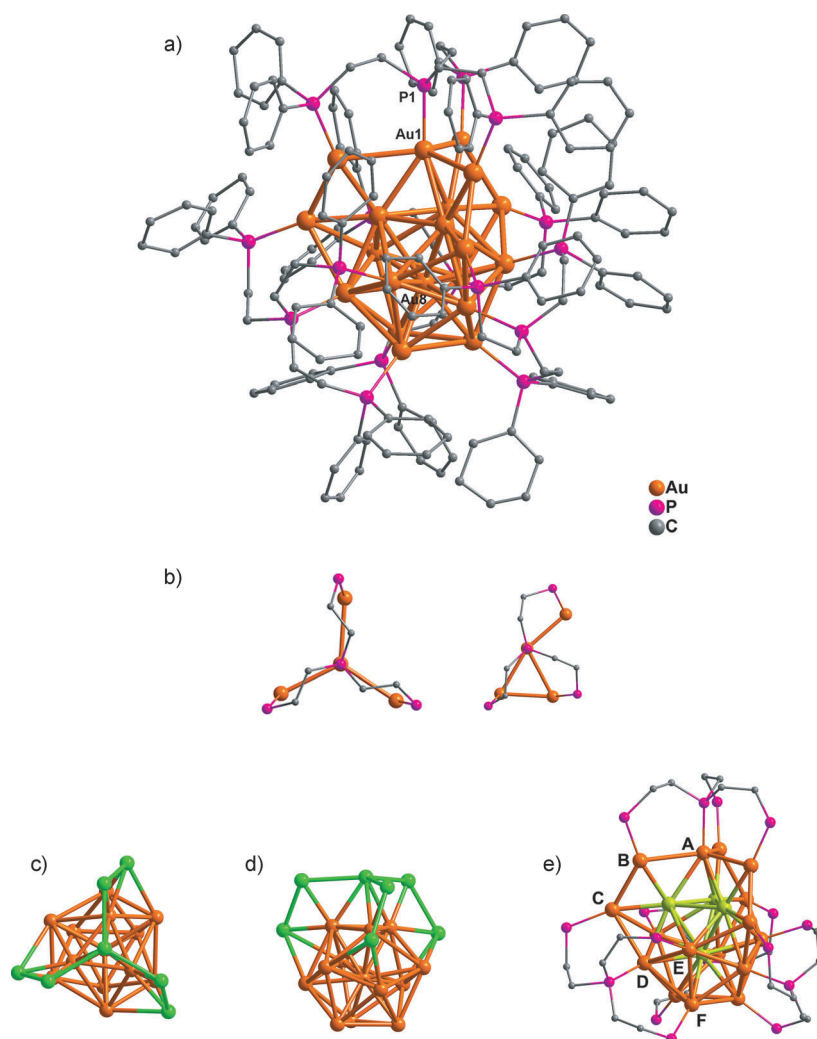


**Figure 1.** a) The structure of the tetracationic  $[\text{Au}_{20}(\text{PP}_3)_4]^{4+}$  cluster in **1**. b) Two types of bridging modes of  $\text{PP}_3$  ligands. c) Top view of the  $\text{Au}_{20}$  core structure in **1**; green atoms denote the  $\text{Au}_7$  unit, and the  $\text{Au}_{13}$  icosahedron is shown in orange; d) side view. e) The bridging mode of  $\text{PP}_3$  in **1**; the 16 surface gold atoms are of six types (from A to F), the four interstitial Au atoms are shown in green, and phenyl groups have been omitted for clarity.

short Au–Au distance of 2.5817(7) Å was found recently in  $[\text{Au}_{14}(\text{PPh}_3)_8(\text{NO}_3)_4]$ .<sup>[16]</sup>

The  $\text{Au}_{20}$  core is chiral. The  $C_3$  symmetry is clearly shown in Figure 1c, where the cluster is viewed down the threefold axis. The helical arrangement of the  $\text{Au}_7$  motif lowers the symmetry of the  $\text{Au}_{20}$  cluster. This is the first structural evidence on a gold nanocluster bearing an intrinsic chiral inorganic core. Previous structurally determined chiral gold nanoclusters all contain achiral inorganic cores in chiral environments, and the origin of the chirality is either the chiral organic ligand or the asymmetric arrangement of staples.

The absolute configuration of **1** is related to the conformation of  $\text{PP}_3$ . Because the flexible  $\text{PP}_3$  can adopt two types of conformations, both enantiomers of **1** are present in the crystal (Supporting Information, Figure S6). Cluster **1** crystallized in a non-centrosymmetric space group, but racemic twinning occurred as suggested by Flack parameter

of 0.36(6). The sample is silent in CD spectroscopy because it is a racemic mixture.

The sample was further characterized by an ESI-TOF mass spectrometer with an electrospray ionization source in positive mode (Figure 2a). The spectrum is quite clean, with the molecular ion peak  $[\text{Au}_{20}(\text{PP}_3)_4]^{4+}$  at  $m/z = 1655.30$  being dominant. A minor peak at  $m/z = 2219.06$  was observed, which corresponds to  $[\text{Au}_{20}(\text{PP}_3)_4\text{Cl}]^{3+}$  derived from the binding of a chloride to  $[\text{Au}_{20}(\text{PP}_3)_4]^{4+}$ . The observed isotopic patterns of  $[\text{Au}_{20}(\text{PP}_3)_4]^{4+}$  and  $[\text{Au}_{20}(\text{PP}_3)_4\text{Cl}]^{3+}$  are perfectly in agreement with the simulated (Figure 2b,c). To fulfill the requirement of charge balance, 16 of the 20 gold atoms should have a valency of zero. The bonding energy of  $\text{Au}4f_{7/2}$  was determined to be 84.3 eV by XPS (Supporting Information, Figure S2), which are characteristic of  $\text{Au}^0$ . Because the Au atoms are largely  $\text{Au}^0$  in the nanocluster, the band at 84.9 eV for  $\text{Au}^{\text{I}}$  could hardly be observed.

Nanoclusters with 20 gold atoms fall in a special category. Wang et al. reported that the most stable form of a bare  $\text{Au}_{20}$  is a tetrahedral ( $T_d$ ) structure.<sup>[17]</sup> They also synthesized ligand-protected  $\text{Au}_{20}$  using a two-phase system, and the product was identified as  $\text{Au}_{20}(\text{PPh}_3)_8^{2+}$  by mass spectrometry, which was computed to have a tetrahedral structure.<sup>[18]</sup> Jin et al. reported a thiolate-protected  $\text{Au}_{20}$  cluster, and its composition  $\text{Au}_{20}(\text{SCH}_2\text{CH}_2\text{Ph})_{16}$  was determined by mass spectrometry.<sup>[19]</sup> Zen et al. theoretically predicted that this thiolate-protected  $\text{Au}_{20}$  cluster has a prolate  $\text{Au}_8$  core with four -RS-Au-RS-Au-RS-Au-RS- extended staples.<sup>[20]</sup> Recently, we reported the first structural determination of a phosphine-protected  $\text{Au}_{20}$  cluster  $[\text{Au}_{20}(\text{PhPpy}_2)_{10}\text{Cl}_2]\text{Cl}_4$ , which has a bivertex-shared double incomplete icosahedral structure.<sup>[21]</sup> The present work represents an unprecedented chiral arrangement of  $\text{Au}_{20}$ .

The UV/Vis absorption spectrum of **1** in  $\text{CH}_2\text{Cl}_2$  shows three prominent absorption bands at 370, 495, 550 (shoulder), and a broad band around 833 nm tailing to 1000 nm (Figure 3). The optical energy gap was determined to be 1.33 eV (Figure 3 inset), which is much lower than 1.77 eV found in bare  $\text{Au}_{20}$ , 2.15 eV in  $\text{Au}_{20}(\text{SCH}_2\text{CH}_2\text{Ph})_{16}$ , and 2.24 eV in  $[\text{Au}_{20}(\text{PhPpy}_2)_{10}\text{Cl}_2]\text{Cl}_4$ . Cluster **1** and  $[\text{Au}_{20}(\text{PhPpy}_2)_{10}\text{Cl}_2]\text{Cl}_4$ <sup>[21]</sup> each contains a phosphine-protected  $\text{Au}_{20}$  core, but they have quite different HOMO–LUMO gaps. This fact shows that the core structures affect the optical properties of gold nanoclusters containing the same number of gold atoms.

Although the optical energy gap of **1** is not high, this  $\text{Au}_{20}$  cluster is quite stable. It is confirmed by UV/Vis spectra that no decomposition was observed after its solution had been

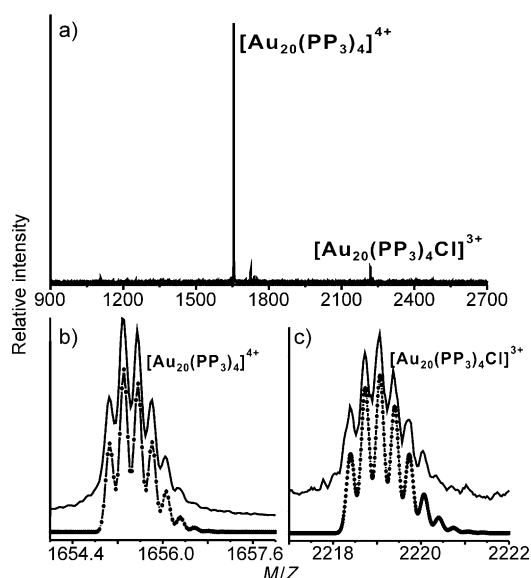


**Figure 2.** a) Mass spectrum of the  $\text{Au}_{20}$  cluster. b), c) The measured (solid trace) and simulated (dotted trace) isotopic patterns of b)  $[\text{Au}_{20}(\text{PP}_3)_4]^{4+}$  and c)  $[\text{Au}_{20}(\text{PP}_3)_4\text{Cl}]^{3+}$ .

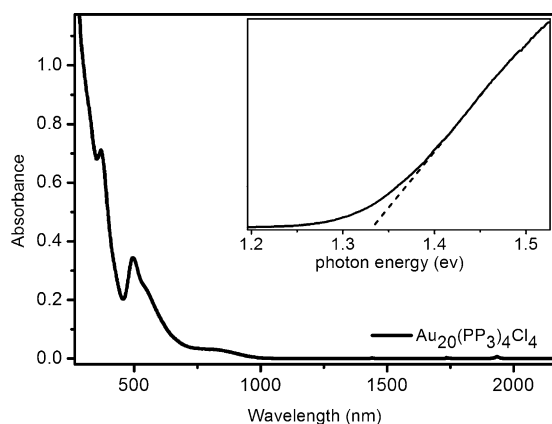


**Figure 3.** The optical absorption spectrum of **1** in dichloromethane. Inset: the spectrum on the energy scale (eV); the HOMO–LUMO gap is 1.33 eV.

stored under ambient conditions in the absence of light for three weeks (Supporting Information, Figure S3). The total number of valence electrons of  $[\text{Au}_{20}(\text{PP}_3)_4]^{4+}$  is calculated to be 16 ( $n=20-4$ ). It does not match either the case of shell closure (18 electrons)<sup>[22]</sup> or the 2D electron-counting requirement (12 electrons).<sup>[23]</sup> The valence electron number of  $\text{Au}_{38}(\text{SR})_{24}$  with a face-fused bi-icosahedral  $\text{Au}_{23}$  core is 14, which is not a magic number as required by the superatom model; this can be explained with an ellipsoidal shell model.<sup>[24,25]</sup> Cluster **1** with a nonspherical structure might also fall in this category. The stability of **1** comes from both electronic and geometrical factors. Furthermore, the chelation of the tetraphosphine  $\text{PP}_3$  provides additional stabilization contribution.

In summary, this work presents important structural evidence on the existence of a chiral gold cluster core. Compound **1** has a new type of  $\text{Au}_{20}$  configuration. The

chelating ability of multidentate phosphines enhances the stability of the  $\text{Au}_{20}$ . The chiral arrangement of the  $\text{Au}_{20}$  core structure indicates that the protecting ligands can impose intense influence on the structure of the resulted gold clusters. We expect that homochiral gold nanoclusters with a chiral inorganic gold core could be prepared with the use of chiral multidentate protecting ligands. Further work on modulating the structures of gold nanoclusters with various bridging ligands is in progress.

### Experimental Section

**Synthesis of 1:** A freshly prepared solution of  $\text{NaBH}_4$  (22.1 mg, 0.585 mmol) in ethanol (3.0 mL) was added dropwise under vigorous stirring to a solution of  $\text{PP}_3\text{Au}_4\text{Cl}_4$  (93.4 mg) in  $\text{CH}_2\text{Cl}_2$  (80 mL). The solution color changed from colorless to brown and finally to black. The reaction mixture was stirred for 10 h at 30 °C in air in the absence of light. Solvent was removed under reduced pressure to give a black solid. This solid was then dissolved in  $\text{CH}_2\text{Cl}_2$  (3.0 mL) and  $\text{CH}_3\text{OH}$  (0.1 mL), and the solution was centrifuged for 4 min at 8000  $\text{r min}^{-1}$ . The brown supernatant was collected and subjected to the diffusion of pentane, black crystals of **1** deposited after about 5 days (17.8 mg, yield 23.2% based on Au).

Received: October 2, 2013

Revised: December 12, 2013

Published online: February 7, 2014

**Keywords:** chiral structures · cluster compounds · gold · nanostructures · phosphines

- [1] G. Li, R. Jin, *Acc. Chem. Res.* **2013**, *46*, 1749–1758.
- [2] H. Häkkinen, *Nat. Chem.* **2012**, *4*, 443–455.
- [3] P. Maity, S. Xie, M. Yamauchi, T. Tsukuda, *Nanoscale* **2012**, *4*, 4027–4037.
- [4] J. F. Parker, C. A. Fields-Zinna, R. W. Murray, *Acc. Chem. Res.* **2010**, *43*, 1289–1296.
- [5] G. Schmid, *Chem. Soc. Rev.* **2008**, *37*, 1909–1930.
- [6] a) C. Gautier, T. Bürgi, *ChemPhysChem* **2009**, *10*, 483–492; b) I. Dolamic, S. Knoppe, A. Dass, T. Bürgi, *Nat. Commun.* **2012**, *3*, 798.
- [7] H. Qian, M. Zhu, Z. Wu, R. Jin, G. Li, R. Jin, *Acc. Chem. Res.* **2012**, *45*, 1470–1479.
- [8] H. Qian, W. T. Eckenhoff, Y. Zhu, T. Pintauer, R. Jin, *J. Am. Chem. Soc.* **2010**, *132*, 8280–8281.
- [9] C. Zeng, T. Li, A. Das, N. L. Rosi, R. Jin, *J. Am. Chem. Soc.* **2013**, *135*, 10011–10013.
- [10] P. D. Jadzinsky, G. Calero, C. J. Ackerson, D. A. Bushnell, R. D. Kornberg, *Science* **2007**, *318*, 430–433.
- [11] a) M. W. Heaven, A. Dass, P. S. White, K. M. Holt, R. W. Murray, *J. Am. Chem. Soc.* **2008**, *130*, 3754–3755; b) M. Zhu, C. M. Aikens, F. J. Hollander, G. C. Schatz, R. Jin, *J. Am. Chem. Soc.* **2008**, *130*, 5883–5885; c) J. Akola, M. Walter, R. L. Whetten, H. Häkkinen, H. Gronbeck, *J. Am. Chem. Soc.* **2008**, *130*, 3756–3757.
- [12] C. Zeng, H. Qian, T. Li, G. Li, N. L. Rosi, B. Yoon, R. N. Barnett, R. L. Whetten, U. Landman, R. Jin, *Angew. Chem.* **2012**, *124*, 13291–13295; *Angew. Chem. Int. Ed.* **2012**, *51*, 13114–13118.
- [13] I. E. Santizo, F. Hidalgo, L. A. Pérez, C. Noguez, I. L. Garzon, *J. Phys. Chem. C* **2008**, *112*, 17533–17539.
- [14] a) K. P. Hall, D. M. P. Mingos, *Prog. Inorg. Chem.* **1984**, *32*, 237–325; b) B. K. Teo, X. Shi, H. Zhang, *J. Am. Chem. Soc.* **1992**, *114*, 2743–2745; c) K. Nunokawa, M. Ito, T. Sunahara, S. Onaka, T. Ozeki, H. Chiba, Y. Funahashi, H. Masuda, T. Yonezawa, H.

- Nishihara, M. Nakamoto, M. Yamamoto, *Dalton Trans.* **2005**, 2726–2730; d) A. Das, T. Li, K. Nobusada, Q. Zeng, N. L. Rosi, R. Jin, *J. Am. Chem. Soc.* **2012**, *134*, 20286–20289; e) Y. Yanagimoto, Y. Negishi, H. Fujihara, T. Tsukuda, *J. Phys. Chem. B* **2006**, *110*, 11611–11614; f) Y. Shichibu, K. Konishi, *Small* **2010**, *6*, 1216–1220.
- [15] Crystal data for **1**: C<sub>168</sub>H<sub>168</sub>Cl<sub>4</sub>P<sub>16</sub>Au<sub>20</sub>,  $a = b = c = 36.0125(2)$  Å,  $V = 46704.6(4)$  Å<sup>3</sup>, cubic, space group  $P\bar{4}3n$ ,  $Z = 8$ ,  $T = 100$  K, 31285 reflections measured, 10933 unique ( $R_{\text{int}} = 0.0741$ ), final  $R1 = 0.1010$ ,  $wR2 = 0.1276$  for 8956 observed reflections [ $I > 2\sigma(I)$ ]. CCDC 959621 (**1**) contains the supplementary crystallographic data for this paper. These data can be obtained free of charge from The Cambridge Crystallographic Data Centre via [www.ccdc.cam.ac.uk/data\\_request/cif](http://www.ccdc.cam.ac.uk/data_request/cif).
- [16] B. S. Gutrath, I. M. Oppel, O. Presly, I. Beljakov, V. Meded, W. Wenzel, U. Simon, *Angew. Chem.* **2013**, *125*, 3614–3617; *Angew. Chem. Int. Ed.* **2013**, *52*, 3529–3532.
- [17] J. Li, X. Li, H.-J. Zhai, L.-S. Wang, *Science* **2003**, *299*, 864–867.
- [18] M. F. Bertino, Z.-M. Sun, R. Zhang, L.-S. Wang, *J. Phys. Chem. B* **2006**, *110*, 21416–21418.
- [19] M. Zhu, H. Qian, R. Jin, *J. Am. Chem. Soc.* **2009**, *131*, 7220–7221.
- [20] Y. Pei, Y. Gao, N. Shao, X. C. Zeng, *J. Am. Chem. Soc.* **2009**, *131*, 13619–13621.
- [21] X.-K. Wan, Z.-W. Lin, Q.-M. Wang, *J. Am. Chem. Soc.* **2012**, *134*, 14750–14752.
- [22] H. Häkkinen, *Chem. Soc. Rev.* **2008**, *37*, 1847–1859.
- [23] M. Water, P. Frondelius, K. Honkala, H. Häkkinen, *Phys. Rev. Lett.* **2007**, *99*, 096102.
- [24] Y. Pei, Y. Gao, X. C. Zeng, *J. Am. Chem. Soc.* **2008**, *130*, 7830–7832.
- [25] K. Clemenger, *Phys. Rev. B* **1985**, *32*, 1359–1362.